Nuclear Magnetic Resonance Studies of Amino Acids and Proteins. Deuterium Nuclear Magnetic Resonance Relaxation of Deuteriomethyl-Labeled Amino Acids in Crystals and in *Halobacterium halobium* and *Escherichia coli* Cell Membranes†

Max A. Keniry, Agustin Kintanar, Rebecca L. Smith, H. S. Gutowsky, and Eric Oldfield*,‡

ABSTRACT: We have obtained deuterium (^{2}H) Fourier transform nuclear magnetic resonance (NMR) spectra of zwitterionic L-[β-$^2H_3$]alanine, DL-[γ-$^2H_6$]valine, DL-[β,γ-$^2H_4$]threonine, L-[δ-$^2H_3$]leucine, and L-[$\alpha,\beta,\gamma,\gamma',\delta$-$^2H_{10}$]isoleucine in the crystalline solid state and have determined the deuteriomethyl group spin–lattice relaxation rates as a function of temperature. The results yield the Arrhenius activation energies ($\Delta E^{\ddagger}$) for methyl rotation, and through use of a suitable mathematical model, rotational correlation times, τ_c. For alanine, valine, threonine, leucine, and isoleucine at 37 °C, τ_c and $\Delta E^{\ddagger}$ values are 780, 100, 40, 38, and 18 ps and 22, 14.0, 17.6, 15.5, and 8.6 kJ, respectively. For L-[β-$^2H_3$]alanine in the zwitterionic lattice, a spin–lattice relaxation time (T_1) minimum of 2.1 ± 0.3 ms is observed (at 0 °C), in excellent agreement with the 1.92-ms prediction of the mathematical model. Similar τ_c and $\Delta E^{\ddagger}$ measurements are reported for bacteriorhodopsin in the purple membrane of *Halobacterium halobium* R_1 and for *Escherichia coli* cell membranes. Overall, our results demonstrate a great similarity between the dynamics in amino acid crystals and in membrane proteins. However, threonine exhibits a nonlinear Arrhenius behavior in bacteriorhodopsin, and in the valine-, leucine-, and isoleucine-labeled membrane samples at higher temperatures (≳37 °C), there is evidence of an additional slow side-chain motion. The lipid phase state in *E. coli* does not appear to influence, on the average, the dynamics of the valine side chains. These results indicate that the sensitivity of the deuterium NMR technique is now adequate to study in moderate detail the dynamics of most types of amino acids in a membrane protein and that adequate sensitivity, in some instances, should be available for the study of individual amino acids in suitably labeled membrane proteins.

In the past 10 years, there has been considerable interest in characterizing methyl group reorientation in crystalline amino acids and peptides and in condensed-phase proteins (Zaripov, 1973; Andrew et al., 1976; Jelinski et al., 1980; Oldfield & Rothgeb, 1980; Kinsey et al., 1981a,b; Batchelder et al., 1982).

Early studies of dynamics were confined to the ^{1}H nucleus, for reasons of sensitivity, but with the more recent availability of high-field superconducting magnets, there has been a renewed interest in studying these systems by means of deuterium (^{2}H) nuclear magnetic resonance (NMR)[1] spectroscopy, using selectively labeled amino acids. Such deuterated species are desirable for a variety of reasons: First, the spin–lattice relaxation (T_1) of the ^{2}H nucleus is overwhelmingly intramolecular, and quadrupolar, in nature. For protons, considerable intermolecular contributions to spin–lattice relaxation generally occur, and separation of inter- and intramolecular effects requires isotopic dilution studies using deuterated compounds. Also, because of spin diffusion (Bloembergen, 1949; McCall & Douglass, 1963; Anderson & Slichter, 1965), proton relaxation is dominated by any "heat sink" present. For example, in solid ribonuclease (EC 2.7.7.16) at 23 °C, the spin–lattice relaxation of virtually all protons is determined by the reorientation of the methyl groups of the molecule (Andrew et al., 1980). In such a situation, study of aromatic ring flipping, for example, would not be possible. By contrast, however, spin diffusion is not significant in ^{2}H NMR studies of selectively labeled species, although some effects could become apparent for massively labeled materials (Alla et al., 1980; Schajor et al., 1980). Finally, we note that selective labeling with ^{2}H permits analysis of the rates and types of motion both of different types of amino acids and of different parts of the same amino acid, in favorable systems. Such analyses are in principle possible with ^{13}C NMR, but for dilute systems, its larger natural abundance gives a background spectrum strong enough to be a significant obstacle.

In this paper, we present our results on the ^{2}H NMR spectroscopy of five ^{2}H-labeled amino acids: L-[β-$^2H_3$]alanine, DL-[γ-$^2H_6$]valine, DL-[β,γ-$^2H_4$]threonine, L-[δ-$^2H_3$]leucine, and L-[$\alpha,\beta,\gamma,\gamma',\delta$-$^2H_{10}$]isoleucine, amino acids which all contain fully deuterated methyl groups. Through the use of a suitable mathematical model, we determine the rotational correlation times of these residues (together with their barriers to rotation) both in the pure, crystalline amino acids and in amino acids (except for alanine) incorporated biosynthetically into the purple membrane of *Halobacterium halobium* R_1. In addition, we discuss preliminary results obtained on [γ-$^2H_6$]valine-labeled *Escherichia coli* cell membranes, enriched with either oleate or elaidate, and on [δ-$^2H_3$]leucine-labeled *E. coli* membranes, systems which may eventually enable us to study the effects of lipids on the dynamic structure of proteins.

† From the School of Chemical Sciences, University of Illinois at Urbana-Champaign, Urbana, Illinois 61801. *Received December 28, 1982; revised manuscript received August 23, 1983.* This work was supported in part by the National Institutes of Health (Grant HL-19481), the National Science Foundation (Grants PCM 79-11148, 79-23170, and 81-17813), and the American Heart Association (Grant 80-867) and has benefited from the use of facilities made available through the University of Illinois–National Science Foundation Regional NMR Instrumentation Facility (Grant CHE 79-16100).

‡ U.S. Public Health Service Research Career Development Awardee, 1979–1984 (Grant CA-00595).

[1] Abbreviations: NMR, nuclear magnetic resonance; T_1, spin–lattice relaxation time; PRFT, partially relaxed Fourier transform; QS, quadrupole splitting; bR, bacteriorhodopsin; TLC, thin-layer chromatography; BPTI, bovine pancreatic trypsin inhibitor.

0006-2960/84/0423-0288$01.50/0

Experimental Procedures

Nuclear Magnetic Resonance Spectroscopy. Deuterium NMR spectra were obtained on two "home-built" Fourier transform NMR spectrometers, operating at 5.0 and 8.45 T (corresponding to ^2H resonance frequencies of 32.9 and 55.3 MHz, respectively), basically as discussed elsewhere (Schramm & Oldfield, 1983) except that the 5.0-T instrument incorporated a Nicolet (Nicolet Instrument Corp., Madison, WI) Model 293 pulse programmer interfaced to a Biomation (Biomation Corp., Cupertino, CA) Model 805 waveform recorder, which allowed sampling of up to 2048 points in the time domain at 1 μs per point. All spectra were recorded by using a quadrupole echo sequence (Davis et al., 1976) with 90° pulse widths of about 3 μs. Spin–lattice relaxation times were determined by using an inversion recovery technique with a recycle time of at least $5T_1$. Typically, 8–10 points were obtained for each inversion recovery experiment and were analyzed with a nonlinear three-parameter fit routine (Levy & Peat, 1975) on a Nicolet 1180 computer system, using the NTCFTB program. Spectral simulations were carried out on the University of Illinois Digital Computer Laboratory's Control Data Corp. Cyber-175 system, as described previously (Kang et al., 1979a). Calculations of correlation times and theoretical fits of the Arrhenius plots were performed on the University of Illinois School of Chemical Sciences Digital Equipment Corp. VAX-11/780.

Labeled Compounds. L-[β-$^2H_3$]Alanine, DL-[α,β,γ-$^2H_8$]-valine, and L-[δ-$^2H_3$]leucine were obtained from Merck Sharp & Dohme (Montreal, Canada), and [$\alpha,\beta,\gamma,\gamma',\delta$-$^2H_{10}$]isoleucine was purchased from Cambridge Isotope Laboratories (Cambridge, MA). After being dried, all were used without further purification. DL-[γ-$^2H_6$]valine was synthesized as described previously (Kinsey et al., 1981b). DL-[β,γ-$^2H_4$]Threonine (~75% in the threo form) was synthesized by condensing [$^2H_4$]acetaldehyde (Merck Sharp & Dohme, Montreal, Canada) with bis(glycine)copper(II) (Sato et al., 1957). Copper was removed on a column of Dowex 50W-X8 (Bio-Rad, Richmond, CA), by using 5 M NH_4OH as the eluant. Solvent was removed under reduced pressure, and the DL-[β,γ-$^2H_4$]threonine was recrystallized from methanol/water (4:1 v/v).

L-[γ-$^2H_6$]Valine was prepared from the DL isomer by cleaving the acetyl group of *N*-acetyl-DL-[γ-$^2H_6$]valine (Fodor et al., 1949) with porcine kidney acylase I (*N*-acylamino-acid amidohydrolase, EC 3.5.1.14; Sigma, St. Louis, MO). L-[γ-$^2H_6$]Valine was separated from the D-acetyl derivative by crystallization several times from aqueous ethanol (Fodor et al., 1949). DL-[δ-$^2H_3$]Leucine was prepared by recrystallizing equimolar amounts of L-[δ-$^2H_3$]leucine and unlabeled D-leucine (Aldrich Chemical Co., Milwaukee, WI) from aqueous ethanol. The hydrochloride form of L-[β-$^2H_3$]alanine was produced by dissolving the zwitteronic form in water at pH 2, removing the solvent under vacuum, and crystallizing the oily residue by adding ethanol and then ether.

The purity of each amino acid was verified by means of two-dimensional thin-layer chromatography (TLC) on 160-μm Eastman-Kodak Chromagram cellulose TLC plates (Rochester, NY) using 2-propanol, 1 M HCl, and 2-butanone (60:25:15 v/v, first dimension) followed by 2-methyl-2-propanol, 2-butanone, acetone, H_2O, 28% NH_4OH, and MeOH (40:20:20:14:5:1 v/v, second dimension) as developers. Visualization was by means of a ninhydrin spray reagent. The purity of all samples was further verified with ^1H NMR spectroscpy at 90, 220, or 360 MHz, and by C, H, and N microanalysis at the Microanalytical Laboratory of the University of Illinois. All samples were dried prior to ^2H NMR spectroscopy, either in an oven or in vacuo over P_4O_{10}. All amino acids were in the zwitterionic form, unless otherwise stated.

Production of ^2H-Labeled Membranes. Halobacterium halobium R_1 was the gift of Professor T. Ebrey and was grown and harvested as described previously (Kinsey et al., 1981a,b). As appropriate, deuterated amino acids were incorporated at the following levels into the growth medium: DL-[γ-$^2H_6$]valine, 10 g/10 L; DL-[β,γ-$^2H_4$]threonine, 5 g/10 L; L-[δ-$^2H_3$]leucine, 0.2 g/5 L; L-[$\alpha,\beta,\gamma,\gamma',\delta$-$^2H_{10}$]isoleucine, 0.2 g/5 L. We assume only L-amino acids are incorporated into the membrane proteins.

The *Escherichia coli* fatty acid auxotroph strain TS1 was the gift of Dr. John Cronan, University of Illinois, Urbana, and was grown on minimal medium E of Vogel & Bonner (1956) supplemented with thiamin (1 μg/mL), succinate (2 mg/mL), uracil (10 μg/mL), oleic or elaidic acid (100 μg/mL), Brij-59 (400 μg/mL), and DL-amino acids (0.1 mg/mL each; except L-proline, 0.2 mg/mL). DL-[γ-$^2H_6$]Valine was substituted for the normal ^1H isomer for production of valine-labeled cell membranes.

The leucine auxotroph 23783 was obtained from the American Type Culture Collection (Rockville, MD). It was grown basically as described above using type E medium, except that L-[δ-$^2H_3$]leucine (0.05 mg/mL) was used instead of the unlabeled leucine and the medium was supplemented with oleate, not elaidate. Growth of *E. coli* and cell membrane (inner plus outer) isolation were as described previously (Kang et al., 1979b).

All membrane samples were exchanged at least 2 times with ^2H-depleted water (Aldrich) and ^2H NMR spectra obtained as soon as possible after pelleting by ultracentrifugation. In general, low-temperature NMR experiments were run first to minimize degradation of the membrane samples.

Radiotracer Experiments. To determine the level of deuterated amino acid breakdown in *H. halobium*, and reincorporation into other amino acids, 1-L batches of cells were grown and harvested basically as for the ^2H-labeled materials, except that 50 μCi of either [^{14}C]Val, [^{14}C]Thr, or [^{14}C]Leu (New England Nuclear, Boston, MA) was added as a radiotracer. Purple membranes were isolated, lyophilized, lipid extracted (3 times with $CHCl_3$/MeOH, 1:2 v/v), and then hydrolyzed in 6 M HCl (24 h at 110 °C, under vacuum). The hydrolysates were chromatographed by using two-dimensional thin-layer chromatography and then visualized and counted for radioactivity as described previously (Kinsey et al., 1981a).

Our results indicate that 100 ± 5% of the radioactivity in the valine and threonine hydrolysates was associated with these amino acids on the two-dimensional chromatogram. With leucine, we obtained a rather poor separation between Leu and Ile: our results indicate that 94 ± 5% of the radioactivity was associated with a Leu-Ile spot and 6 ± 2% with a Phe spot. The Leu-Ile spot apparently contained about one-fourth of the counts in the Ile position and three-fourths in the Leu position. However, we believe these results are due primarily to incomplete resolution and that ~100 ± 10% of the [^{14}C]Leu radioactivity is associated with leucine, i.e., there is essentially no breakdown. We have not performed radiotracer experiments on isoleucine, although the ^2H NMR results suggest that the deuterons remain in the methyl groups.

We should add at this point that although we have now reported little breakdown of Val, Thr, Leu, Phe, Tyr, and Trp (Kinsey et al., 1981a,b), upon their incorporation into *H. halobium* R_1, many other amino acids *are* modified, including

alanine, aspartic acid, glutamic acid, glycine, methionine, proline, and serine (J. Nichols, J. Vandenbranden, B. Montez, R. L. Smith, and E. Oldfield, unpublished results). Thus, it is far from being axiomatic that amino acid incorporation into the purple membrane of *H. halobium* will always proceed smoothly.

Radiotracer experiments with *E. coli* were not carried out since there is considerable evidence that under the growth conditions used there is good incorporation and little breakdown, if any, of Val, Thr, and Leu (J. Cronan, private communication).

Results and Discussion

Theoretical Aspects. Deuterium NMR is dominated by the nuclear electric quadrupole interaction, and the appropriate NMR theory describing this interaction has been discussed in detail previously (Kinsey et al., 1981a). For a deuteron in a methyl group undergoing fast ($>10^7$ s^{-1}) reorientation, the spectra are axially symmetric powder patterns with a quadrupolar splitting $[3e^2qQ/(4h)]$ of ~40 kHz (Kinsey et al., 1981b). The quadrupolar splitting may be narrowed further by libration or hopping of the amino acid side chain. The latter case may result in axially asymmetric line shapes, as has been observed in [$^2H_{10}$]leucine-labeled collagen fibrils by Batchelder et al. (1982).

The NMR relaxation behavior of deuterons is also due to quadrupole effects. The spin–lattice relaxation time (T_1) may be related to the correlation time for the motion by an appropriate mathematical model. The details of the model depend on the *type* of motion, and Torchia & Szabo (1982) have developed models for reorientation of a methyl group by free rotational diffusion and by 3-fold jumps. The former model predicts a single T_1 over the entire powder pattern in the extreme narrowing limit, while the 3-fold jump model produces an orientation-dependent spin–lattice relaxation time.

We have chosen the three-site jump model to analyze our T_1 results and extract correlation times by using the following equation (Torchia & Szabo, 1982):

$$\frac{1}{T_1} = \frac{\omega_Q^2}{8}\left\{\frac{\tau_c}{1+\omega_0^2\tau_c^2}[\sin^2 2\beta\,(\cos^2\theta + \cos^2 2\theta) + \sin^4\beta\,(\sin^2\theta + 0.25\sin^2 2\theta) - 8\sin^3\beta\cos\beta\sin^3\theta\cos\theta\cos 3\phi] + \frac{\tau_c}{1+4\omega_0^2\tau_c^2}[4\sin^2 2\beta\,(\sin^2\theta + 0.25\sin^2 2\theta) + \sin^4\beta(1 + 6\cos^2\theta + \cos^4\theta) + 8\sin^3\beta\cos\beta\sin^3\theta\cos\theta\cos 3\phi]\right\} \quad (1)$$

where $\omega_Q = 3e^2qQ/(4\hbar)$, ω_0 is the nuclear Larmor frequency, τ_c is the jump correlation time, θ and ϕ are the polar angles that describe the orientation of the rotation axis (R) with respect to the external magnetic field, and β is the angle between the rotation axis R and the field gradient tensor, as shown in Figure 1.

The justification for the choice of this model may be seen in Figure 2, which shows representative partially relaxed Fourier transform (PRFT) NMR spectra, at 37 °C, of solid polycrystalline L-[β-$^2H_3$]alanine, DL-[γ-$^2H_6$]valine, DL-[β,γ-$^2H_4$]threonine, and L-[δ-$^2H_3$]leucine, all obtained by using an inversion recovery quadrupole echo pulse sequence. It is apparent from inspection of these spectra that the outer shoulders of each set of PRFT spectra relax faster than the major singularities. This is the result expected on the basis of the angular dependence relationships expressed above. Differential

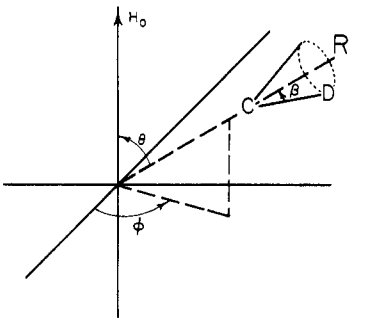

FIGURE 1: Geometry of an isolated deuteriomethyl group oriented with its 3-fold axis inclined at the polar coordinates (θ,ϕ) with respect to the laboratory frame.

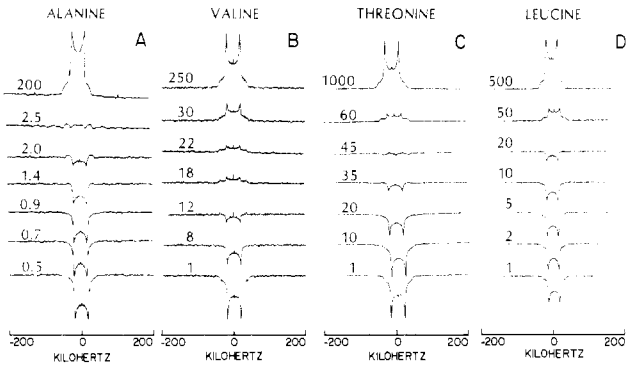

FIGURE 2: Partially relaxed deuterium inversion recovery quadrupole echo Fourier transform NMR spectra of polycrystalline L-[β-$^2H_3$]-alanine, DL-[γ-$^2H_6$]valine, DL-[β,γ-$^2H_4$]threonine, and L-[δ-$^2H_3$]leucine, at 37 °C. (A) Ala at 32.9 MHz, 3-μs 90° pulse widths, $\tau_2 = \tau_3 = 100$ μs, 2-MHz data acquisition rate, 2048 data points, 50 scans per spectrum, line broadening = 500 Hz. (B) Val; same as (A) but 5 scans per spectrum. (C) Thr at 55.3 MHz; same as (A) but $\tau_2 = \tau_3 = 50$ μs and 28 scans per spectrum. (D) Leu; same as (C) but 60 scans per spectrum. The τ_1 values in the PRFT experiment are given on the figure in milliseconds.

T_1 values were also observed in the PRFT's of membrane samples (Figure 6) although the anisotropy is not as apparent because of the more complicated line shapes in these samples.

We have chosen to measure relaxation times at the "singularity" or "90° edge" of the powder spectrum. Only those molecules with $\theta = 90°$ or 35.3° make contributions to this feature, these orientations occurring in the ratio 1:0.58. In order to interpret our relaxation data, we note that in the extreme narrowing limit ($\omega_0\tau_c \ll 1$) ϕ dependence is eliminated. Furthermore, for a methyl group, $\beta = 70.5°$; thus, the resultant simplified T_1 expression has only angular dependence in θ (Torchia & Szabo, 1982) as follows:

$$\frac{1}{T_1} = \frac{4\omega_Q^2\tau}{9}(1 + \cos^2\theta) \quad (2)$$

Substitution into eq 2 yields

$$\frac{1}{T_1}(90°) = \frac{4}{9}\omega_Q^2\tau \quad (3)$$

$$\frac{1}{T_1}(35.3°) = \frac{4}{9}\omega_Q^2\tau(1.67) \quad (4)$$

The T_1 value we observe at the major singularity will be the weighted average of the spin–lattice relaxation times of the two contributing orientations, as follows:

$$\frac{1}{T_1}(\text{obsd}) = \frac{4}{9}\omega_Q^2\tau_c[1 + 0.58(1.67)]/1.58 \quad (5)$$

We used eq 5 to analyze all T_1 results except those for zwitterionic L-[β-$^2H_3$]alanine, where experimental points in the slow-motion regime ($\omega_0\tau_c \gg 1$) are observed. In this case,

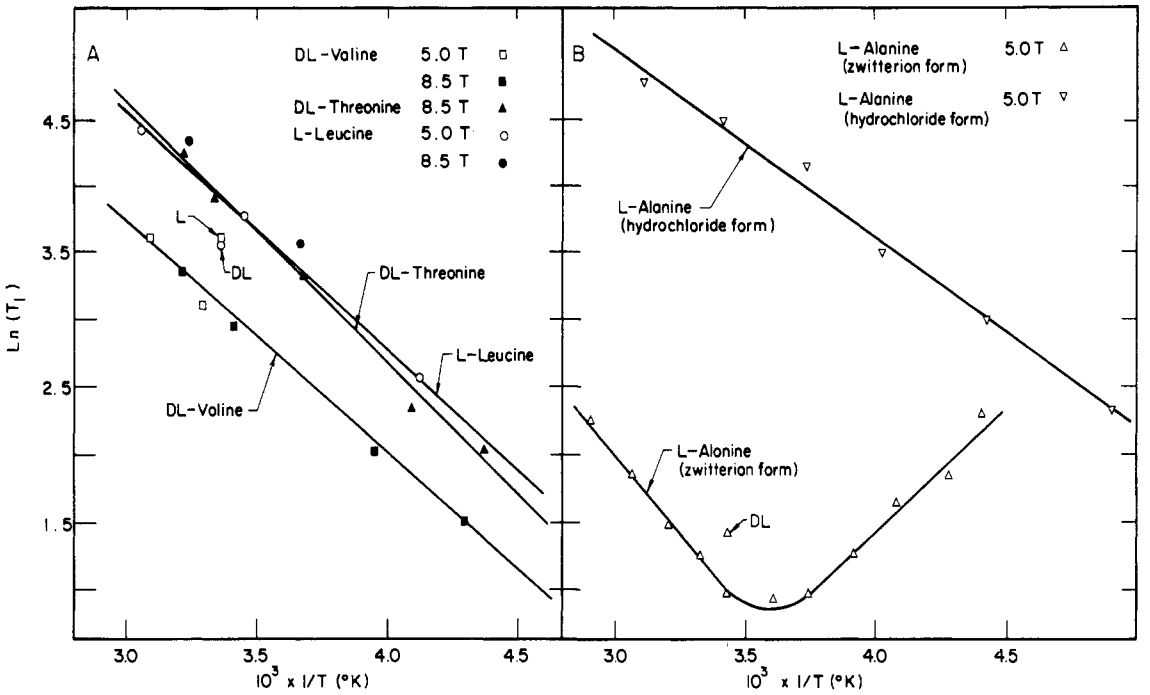

FIGURE 3: (A) Arrhenius plots showing the variation of the ^2H spin–lattice relaxation time (in milliseconds) with inverse temperature for Val, Thr, and Leu (see Table II). Val at 32.9 MHz (□), Val at 55.3 MHz (■), Thr at 55.3 MHz (▲), Leu at 32.9 MHz (○), Leu at 55.3 MHz (●). The plots yield activation energies of 14.0, 17.6, and 15.5 kJ for Val, Thr, and Leu, respectively. (B) Arrhenius plots of the spin–lattice relaxation times (in milliseconds) for the zwitterionic (△) and hydrochloride (▽) forms of L-[β-$^2H_3$]alanine. The plots yield activation energies of 22 and 12.5 kJ for the zwitterionic and hydrochloride forms, respectively.

Table I: Experimental Deuterium NMR Quadrupolar Splittings (QS), Spin–Lattice Relaxation Times (T_1), and Computed Correlation Times (τ_c) for Methyl Rotation in the Polycrystalline Zwitterionic Form of L-[β-$^2H_3$]Alanine and the Hydrochloride Form of L-[β-$^2H_3$]Alanine as a Function of Temperature[a]

L-[β-$^2H_3$]alanine, zwitterionic form				L-[β-$^2H_3$]alanine, hydrochloride form			
temp[b] (°C)	QS[c] (kHz)	T_1 (ms)	τ_c (ps)	temp (°C)	QS[c] (kHz)	T_1 (ms)	τ_c (ps)
70	40	8.4	335	48	40	121	23
38	40	3.9	780	19	40	90	31
18	40	2.3	1510	−5	40	62	45
−7	40	2.3	4000	−26	40	33	85
−28	40	4.6	14000	−47	40	20	139
−46	40	8.8	28000	−69	40	10	289
18	39	4.3[d]	660				

[a] Data obtained by using an inversion recovery quadrupole echo sequence at 5.0 T, corresponding to a ^2H resonance frequency of 32.9 MHz. T_1 and τ_c accuracies are about ±10%. See Figure 3B for Arrhenius curves. [b] Data obtained at 52, 26, −30, and −40 °C are consistent with those at the temperatures given. [c] Obtained from spectral simulation; error is about ±2.5%. [d] T_1 value for zwitterionic form of DL-[β-$^2H_3$]alanine at 5.0 T.

the results were analyzed by using the full expression (eq 1) instead of eq 2, and we averaged over all values of ϕ to eliminate the ϕ dependence of the 35.3° orientation.

The above results predict a nonexponential recovery of the magnetization. Since the probabilities of $\theta = 35.3°$ and 90°, and their corresponding T_1 values are quite close, observation of such nonexponential recoveries will be most difficult, and we have not in fact observed them, although as noted earlier, θ-dependent relaxation is clearly seen in the wings of the ^2H powder spectra (near $\theta = 0°$).

Amino Acids. We have obtained spin–lattice relaxation times as a function of temperature for L-[β-$^2H_3$]alanine, DL-[γ-$^2H_6$]valine, DL-[β,γ-$^2H_4$]threonine, L-[δ-$^2H_3$]leucine, and L-[$\alpha,\beta,\gamma,\gamma',\delta$-$^2H_{10}$]isoleucine, in the crystalline solid state. In the case of alanine, we obtained data for both the HCl and zwitterionic forms; all other amino acids were in the zwitterionic forms only. Our results are shown in Figure 3 and in Tables I and II.

We observe a T_1 minimum for the zwitterionic form of L-[β-$^2H_3$]alanine at about 0 °C, the highest temperature T_1 minimum due to methyl group rotation we have observed in any amino acid. The magnitude of T_1 at the minimum is 2.1 ± 0.3 ms, in excellent agreement with the theoretical prediction of 1.92 ms, strongly supporting our use of the theoretical model outlined above. We assume that the correlation time follows a simple activation law:

$$\tau_c = \tau_0 \exp\left(\frac{\Delta E^\ddagger}{kT}\right) \tag{6}$$

which thus allows us to extract an activation energy ($\Delta E^\ddagger$) and a preexponential time factor (τ_0) of 22 kJ and 2.0×10^{-13} s, respectively, for methyl rotation of alanine in the zwitterionic lattice. Our T_1 results and analysis agree favorably with the solid-state ^1H NMR relaxation results of Zaripov (1973) and Andrew et al. (1976), who find low-temperature relaxation minima due to methyl rotation in zwitterionic Ala at ~−5 °C (27.5 MHz) and 16 °C (60.2 MHz), and the recent ^2H NMR results of Batchelder et al. (1983), who also find a ^2H NMR minimum at ~5 °C (38.5 MHz). Differentiation of eq 1 yields $\omega_0\tau_c \approx 0.6$, from which we can calculate, a priori, correlation times at the minima. The data from the four

Table II: Experimental Deuterium NMR Quadrupolar Splittings (QS), Spin–Lattice Relaxation Times (T_1), and Computed Correlation Times (τ_c) for Methyl Rotation in Polycrystalline Zwitterionic DL-[γ-$^2H_6$]Valine, DL-[β,γ-$^2H_4$]Threonine, L-[δ-$^2H_3$]Leucine, and L-[$\alpha,\beta,\gamma,\gamma',\delta$-$^2H_{10}$]Isoleucine as a Function of Temperature[a]

DL-[γ-$^2H_6$]valine[b]				DL-[β,γ-$^2H_4$]threonine[c]				L-[δ-$^2H_3$]leucine				L-[$\alpha,\beta,\gamma,\gamma',\delta$-$^2H_{10}$]isoleucine[c]			
temp (°C)	QS[d] (kHz)	T_1 (ms)	τ_c (ps)	temp (°C)	QS[d] (kHz)	T_1 (ms)	τ_c (ps)	temp (°C)	QS[d] (kHz)	T_1 (ms)	τ_c (ps)	temp (°C)	QS[d] (kHz)	T_1 (ms)	τ_c (ps)
37	38	29.3	99	37	39	70.6	40	52	31	84.4[b]	34	37	38	162	18
22	39	19.9	140	26	39	52.7	53	35	33	76.3[c]	38	21	38	136	21
−20	39	7.7	370	−1	39	28.0	100	16	34	43.7[b]	65	3	38	105	27
−42	40	4.7	620	29	39	10.4	281	0	35	35.6[c]	83	−16	38.5	82.0	35
20	39	35.5[e]	80	−44	39	6.9	432	−30	36.5	13.0[b]	230	−36	39	57.5	50
36	39	28.9[f]	98					20	36	34.5[g]	85				

[a] T_1 determinations were made by using an inversion recovery quadrupole echo sequence, as described in the text. Signal intensities were measured at the spectral singularity. T_1 and τ_c accuracies are about ±10–20%. See Figures 2 and 3 for typical signal to noise ratios and Arrhenius plots. [b] Data obtained at 5.0 T, corresponding to a ^2H resonance frequency of 32.9 MHz. [c] Data obtained at 8.45 T, corresponding to a ^2H resonance frequency of 55.3 MHz. [d] Obtained from a spectral simulation; error is about ±2.5%. [e] T_1 value for L-[γ-$^2H_6$]-valine, at 5.0 T. [f] T_1 value for DL-[α,β,γ-$^2H_8$]valine, at 5.0 T. [g] T_1 value for L-[δ-$^2H_3$]leucine in a DL lattice, at 5.0 T.

independent T_1 minimum determinations are well described by eq 6 using our experimentally determined τ_0 and $\Delta E^\ddagger$ values, which are also in agreement with those determined by Andrew et al. (1976), who find $\Delta E^\ddagger = 22.5$ kJ and $\tau_0 = 1.5 \times 10^{-13}$ s.

Note that when the sample temperature is decreased below ~−50 °C,there are severe spectral distortions (Figure 4) in the ^2H NMR spectra of zwitterionic L-[β-$^2H_3$]alanine due to an "intermediate exchange" situation (Spiess & Sillescu, 1981) in which the methyl rotation rate is close to e^2qQ/h (~100 kHz). Loss of signal intensity and severe spectral distortions are seen in this regime, which fortunately is sufficiently removed from the methyl T_1 minimum so as not to affect our test of the theoretical predictions.

At sufficiently low temperatures (~−135 °C, Figure 4), the rate of methyl rotation is slowed down enough to give a normal "rigid-lattice" ^2H NMR spectrum of L-[β-$^2H_3$]alanine, which displays a quadrupole splitting of ~128 kHz, corresponding to an e^2qQ/h value of 171 ± 5 kHz (Figure 4). A similar result has been obtained independent of this work by Batchelder et al. (1983).

Correlation times calculated by using the methyl group spin–lattice relaxation rates and the jump model described above are given in Table I for Ala in the zwitterionic and hydrochloride forms and in Table II for Val, Thr, Leu, and Ile in the zwitterionic form.

The analysis of the relaxation data in terms of a single correlation time is clearly a good approximation for alanine, valine, and threonine, where the ^2H resonances show a quadrupolar splitting (~38 kHz) and an asymmetry parameter ($\eta \sim 0$) characteristic of methyl rotation, but it could be less valid for isoleucine, which has two different methyl groups, and for leucine at higher temperatures, where the ^2H quadrupolar splitting is slightly smaller (~34 kHz at 37 °C). This small decrease in quadrupolar splitting may be accounted for by libration of the side chain within a cone having a semiangle ≲12° (Batchelder et al., 1982). In any case, such a small-amplitude motion, even if it were occurring at the most efficient frequency for relaxation (i.e., the Larmor frequency), would be unlikely to cause any significant deviation in the relaxation behavior, and indeed, we observed a linear Arrhenius plot for solid, zwitterionic L-[$^2H_3$]leucine.

We believe that methyl rotation is the dominant relaxation mechanism for all of the solid deuterated amino acids over the temperature range examined in this paper. We should point out that other amino acids may be much less well-behaved, as is discussed for the case of methionine in a previous publication (Keniry et al., 1983). Moreover, this may not be the case in the more complicated systems, such as a membrane protein, where a greater range of motions may be expected to occur.

Amino Acid Dynamics: Correlation Times. The results of Figures 2 and 3 and Tables I and II indicate that there appears to be a gradient of motion along the amino acid side chain, with τ_c decreasing as the site of ^2H label incorporation becomes progressively distal to the C^α "backbone" (although we are of course dealing with only a small set of values). For example, for the zwitterionic forms of Ala, Val, Thr, Leu, Ile, and Met (Keniry et al., 1983), τ_c values for methyl rotation decrease in the solid amino acid at 37 °C as follows:

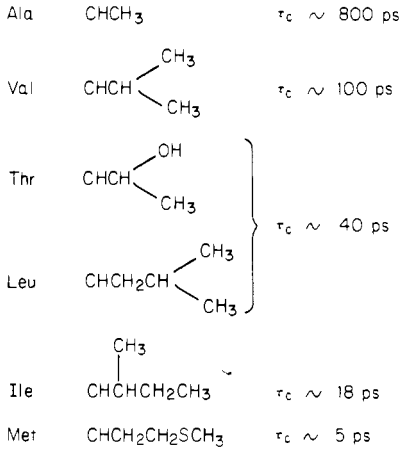

It seems reasonable to postulate that the decreased rotational correlation times observed upon increasing the length of the amino acid side chain are due to decreased barriers to methyl rotation. The very long correlation time of alanine is due either to a large barrier to methyl rotation because of the proximity of the $-CO_2^-$ and $-NH_3^+$ substituents on C^α or to the presence of methyl–methyl contacts in the crystal (Batchelder et al., 1983), or to a combination of both effects. The extremely rapid motion of methionine (Keniry et al., 1983) is due to the very low barrier to rotation in the thioether fragment. For Val, Thr, and Leu, there appears to be a slight increase in the rate of motion with decreased substitution at C^β (Val → Thr) or insertion of a methylene group (Val → Leu) (Table II), but at lower temperatures, this behavior is less apparent (Figure 3).

The results for isoleucine are much more difficult to analyze since it contains two kinds of deuterated methyl groups, as well as labels at the α, β, and γ-carbon positions. Elucidation of the detailed dynamics of the isoleucine side chain awaits experiments with the appropriate selectively labeled compounds

Table III: Experimental Arrhenius Activation Energies for ^1H and ^2H Amino Acids as Polycrystalline Solids and Incorporated into *H. halobium* R_1 and *E. coli* Cell Membranes and *E. coli* Alkaline Phosphatase Crystals[a]

	$\Delta E^{\ddagger}$ (kJ) for				
	alanine	valine	threonine	leucine	isoleucine
crystals[b]	22.9 (L)	14.0 (DL)	17.2 (DL)	15.4 (L)	8.6 (L)
H. halobium, ^2H[c]	nm[d]	10.1 (L)	19.7 (L)[e]	11.3 (L)	7.7 (L)
E. coli, ^2H[f]	nm[d]	9.6 (L)	nm[d]	14.7 (L)	nm[d]
alkaline phosphatase, ^2H[g]	nm[d]	9.0 (L)	nm[d]	7.4 (L)	nm[d]
crystals, ^1H[h]	22.4 (L)	11.3 (L)	12.0 (L)	13.0 (L)	13.2 (DL)
polyamino acid[i]	10.5 (L)	8.5 (L)	nm[d]	8.0 (L)	nm[d]

[a] Activation energies all have an uncertainty of approximately ±10%. [b] These values were determined as described in the text (see Figure 3). [c] As in footnote *b*, but the amino acids were incorporated into bacteriorhodopsin in the purple membrane of *Halobacterium halobium* R_1. See Figures 6 and 7 for experimental results. [d] Not measured. [e] Data for [β,γ-$^2H_4$]threonine were fitted to a double exponential; the value shown is the high-temperature value (≳10 °C). [f] Typical recovery curves are shown in Figure 9. [g] Alkaline phosphatase (EC 3.3.3.3) crystals in 70% saturated $(NH_4)_2SO_4$. [h] Data obtained from Andrew et al. (1976). [i] Data obtained from Andrew et al. (1978).

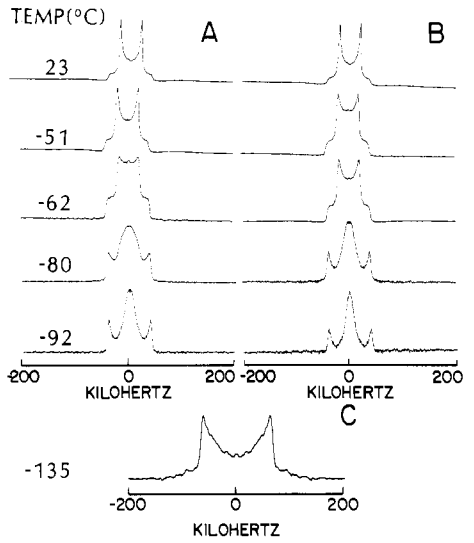

FIGURE 4: Distortion of the ^2H NMR line shape of L-[β-$^2H_3$]alanine at lower temperatures where $1/\tau_c \approx e^2qQ/h$ (100 kHz). Spectra were obtained at 55.3 and 32.9 MHz (8.45 and 5.0 T, respectively) by means of a quadrupole echo pulse sequence. Top spectra (A and B) were obtained at 55.3 MHz by using 3-μs 90° pulse widths, $\tau_1 = \tau_2 = 50$ μs (A, at left) or $\tau_1 = \tau_2 = 100$ μs (B, at right), 2-MHz digitization rate, 2048 data points, 400-Hz line broadening, 50 scans per spectrum, and a recycle time of between 0.5 and 2 s. Sample temperatures are shown in degrees centrigrade. Slow methyl rotation, at an intermediate exchange rate, causes severe spectral distortions (Spiess & Sillescu, 1981). (C) The bottom spectrum was taken at −135 °C (at 32.9 MHz) and displays the full rigid lattice breadth corresponding to an e^2qQ/h of ~171 ± 5 kHz.

or the results of natural-abundance ^{13}C NMR studies.

The restricted motion of amino acid side chains has been investigated previously in solution by numerous workers [see Williams (1978) and references cited therein and Karplus & McCammon (1981)]. However, lattice-packing effects may be significant in the solid state, and additional experiments need to be carried out to determine their importance. Also, the onset of additional modes of motion at high temperature may cause more rapid relaxation in systems like leucine (and methionine). Therefore, observations of differences in the motional behavior of the methyl group will in general best be made at low temperatures, where methyl rotation is the overwhelmingly dominant relaxation process.

Our results with several L,DL amino acid pairs (Tables I and II; Keniry et al., 1983; A. Kintanar et al., unpublished results) indicate that lattice packing has a significant effect on the dynamics of amino acid side chains. We find that the correlation times of the L and DL forms may differ by as much as a factor of 3, and in some cases, large-amplitude motions of the side chain are suppressed completely within the temperature range studied, as is the case for methionine (Keniry et al., 1983). Similar differential motional behavior in the L and DL lattice has been observed by Zaripov (1973).

We may also vary the lattice packing by altering the charge state of the amino acid. The methyl correlation times of the hydrochloride form of L-alanine are similar to those of the zwitterionic form of Val, Thr, and Leu (Tables I and II) but are more than an order of magnitude faster than that for the zwitterionic form of Ala. Moreover, we observe no T_1 minimum for the hydrochloride form, in contrast to our results obtained on the zwitterionic form of L-Ala. Different motional behavior between the zwitterionic and hydrochloride forms of phenylalanine has also been observed, except in this case the zwitterionic form has ring-flip correlation times about 5 orders of magnitude faster than in the HCl lattice and there is a T_1 minimum in the former but not in the latter.

Clearly, caution must be exercised when investigating the dynamics of the various methyl-containing amino acids to ensure that similar lattice types are being compared. Nevertheless, our results still support the idea of increased motional freedom upon increasing side-chain length. For example, for zwitterionic L-Ala, L-Val, and L-Leu at ~20 °C, τ_c decreases from 1500 to 80 to ~60 ps, while for zwitterionic DL-Ala, DL-Val, and DL-Leu, also at ~20 °C, τ_c decreases from 660 to 140 to 85 ps. A more detailed understanding of the effect of lattice packing on dynamics awaits high-resolution X-ray or neutron diffraction studies of the various amino acid crystal lattice forms and the results of molecular dynamics simulation studies.

Amino Acid Dynamics: Activation Energies. Further analysis of the molecular dynamics of methyl groups in amino acids may be based on activation energies ($\Delta E^{\ddagger}$) as obtained from Arrhenius (ln T_1 vs. T^{-1}) relaxation plots. The Arrhenius plots of the relaxation times for methyl groups in the deuterated, polycrystalline amino acids shown in Figure 3 are linear and yield activation energies ($\Delta E^{\ddagger}$) for the motion (methyl rotation) causing relaxation. The $\Delta E^{\ddagger}$ values obtained (Table III) are as follows: L-[β-$^2H_3$]alanine, 22.0 ± 1 kJ; DL-[γ-$^2H_6$]valine, 14.0 ± 1 kJ; DL-[β,γ-$^2H_4$]threonine, 17.0 ± 1.8 kJ; L-[δ-$^2H_3$]leucine, 15.5 ± 1.5 kJ; L-[α,β,γ,γ′,δ-$^2H_{10}$]isoleucine, 8.6 ± 1 kJ. Also shown in Table III are additional activation energy parameters for ^2H-labeled *H. halobium* R_1 and *E. coli* cell membranes and also for alkaline phosphatase (S. Schramm and E. Oldfield, unpublished results), the latter as microcrystals from ammonium sulfate solution.

We must exercise caution, however, when trying to draw conclusions from the activation energy results, since we are comparing both L and DL lattices, and lattice-packing effects may in some cases affect the activation energy (Zaripov, 1973).

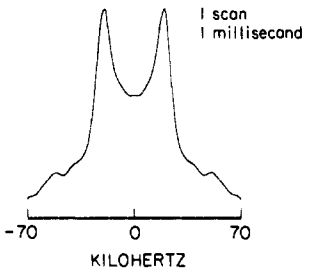

FIGURE 5: Deuterium quadrupole echo Fourier transform NMR spectrum of [γ-$^2H_6$]valine biosynthetically incorporated into the purple membrane of *H. halobium* R_1 in excess water at ~−100 °C. The spectrum arises from the 21 valines in the purple membrane protein (~126 deuterons). Spectral conditions are basically as in Figure 4 except only one scan was necessary and a 1-kHz line broadening was applied. Total acquisition time was 1 ms.

Nevertheless, the activation energies we observe roughly follow the trend of less restricted methyl motion as we move out along the side chain, with the exception of isoleucine and valine. The activation energy for isoleucine is much lower than that for any of the other crystalline, zwitterionic amino acids we have observed. This may be a consequence of there being a distribution of correlation times which may result in an underestimate of $\Delta E^{\ddagger}$. The activation energy of valine is too low to be in accord with the aforementioned trend. This illustrates another problem in using activation energies to estimate mobility, since it is the overall free energy of activation, and not just the Arrhenius activation energy, that determines the rate of a reaction (Glasstone et al., 1941). Equation 6 should thus be recast in the form

$$\tau_c = \frac{h}{kT}\exp\left(\frac{\Delta G^{\ddagger}}{RT}\right) = \frac{h}{kT}\exp\left(\frac{\Delta H^{\ddagger}}{RT} - \frac{\Delta S^{\ddagger}}{R}\right) \quad (7)$$

where $\Delta G^{\ddagger}$, $\Delta H^{\ddagger}$, and $\Delta S^{\ddagger}$ are the free energy, enthalpy, and entropy of activation, respectively. Since $\Delta H^{\ddagger} \approx \Delta E^{\ddagger}$ in condensed phases (Glasstone et al., 1941), it is the activation entropy ($\Delta S^{\ddagger}$) which can cause deviations from the elementary reaction rate theory described by eq 6. Comparison of eq 6 and eq 7 shows that the preexponential time factor, τ_0, is approximately $[h/(kT)][\exp(-\Delta S^{\ddagger}/R)]$ instead of $h/(kT)$ predicted by the rate theory for reactions in the gas phase.

Fortunately, we may calculate $\Delta S^{\ddagger}$ if we know the correlation time, which we can obtain from eq 5. We thus calculate activation entropies of −3.8, +0.5, and −1.0 eu for DL-valine, DL-threonine, and L-leucine, respectively. Note the large negative entropy of activation for DL-[γ-$^2H_6$]valine. This effect is enough to account for the relatively long correlation time observed, despite the low barrier to methyl rotation.

Protein Dynamics: Bacteriorhodopsin. Deuterium FT NMR spectra of [γ-$^2H_6$]valine incorporated into bacteriorhodopsin of the purple membrane of *H. halobium* R_1 were reported by us recently (Kinsey et al., 1981b). With improved instrumentation, we have now obtained spectra with good signal to noise ratios in even shorter periods of time than those required previously. A representative spectrum of [γ-$^2H_6$]-valine-labeled purple membrane, obtained in only 1 ms, is shown in Figure 5. Such short data acquisition periods are exceptional, since we are observing some 126 deuterons with small quadrupole splittings, but the results of Figure 5 do suggest that time-resolved photochemical studies by NMR on purple membrane may not be too far away.

More representative deuterium PRFT spectra for [γ-$^2H_6$]valine-, [β,γ-$^2H_4$]threonine-, [δ-$^2H_3$]leucine-, and [$\alpha,\beta,\gamma,\gamma',\delta$-$^2H_{10}$]isoleucine-labeled *H. halobium* purple membranes are shown in Figure 6 [the valine results are from Kinsey et al. (1981b)]. The ^2H NMR spectra of [β,γ-$^2H_4$]threonine-labeled purple membrane have essentially the same quadrupole splittings (QS) and asymmetry parameters (η) as the ^2H NMR spectra of the pure polycrystalline amino acid (Figures 2 and 6 and Tables I, II, and IV). The spectra of [γ-$^2H_6$]valine-, [δ-$^2H_3$]leucine-, and [$\alpha,\beta,\gamma,\gamma',\delta$-$^2H_{10}$]isoleucine-labeled purple membranes, however, are not well simulated by the characteristic ($\eta \sim 0$, QS ~ 40 kHz) powder pattern of rotating methyl groups, especially at temperatures above 0 °C. These spectra may be simulated by assuming that some or all of the side chains of these methyl-containing residues are undergoing hops between two and four possible conformations. Such side-chain hopping, in addition to fast methyl rotation, gives

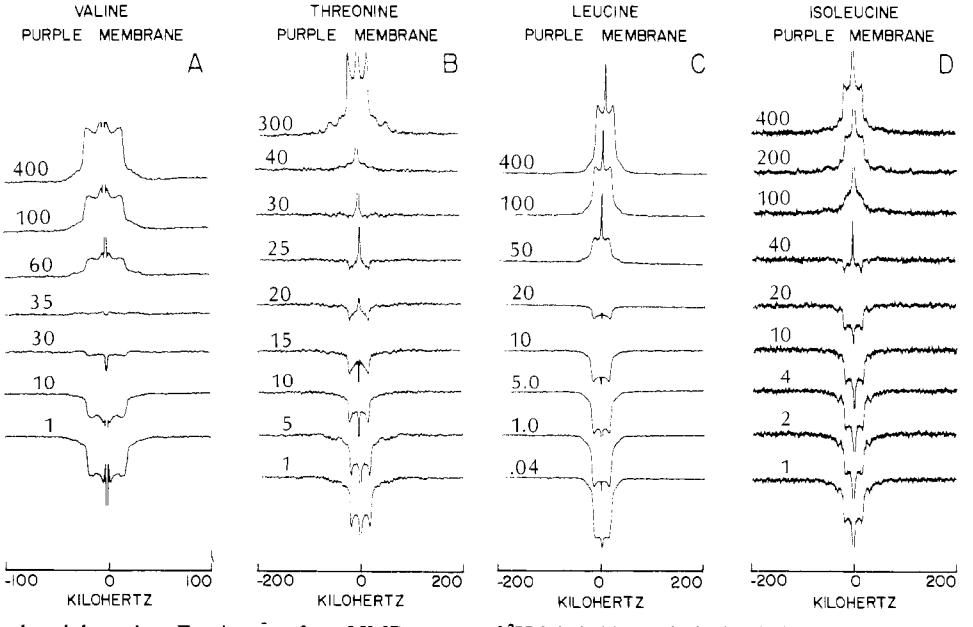

FIGURE 6: Partially relaxed deuterium Fourier transform NMR spectra of ^2H-labeled bacteriorhodopsin in the purple membrane of *H. halobium* R_1 obtained at 55.3 MHz (corresponding to a magnetic field strength of 8.45 T), at 37 °C in excess ^2H-depleted water. (A) [γ-$^2H_6$]Valine, 3-μs 90° pulse widths, $\tau_2 = \tau_3 = 50$ μs, 2-MHz digitization rate, 2048 data points, 500-Hz line broadening, 2000 scans per spectrum, recycle time = 2 s. (B) [β,γ-$^2H_4$]Threonine, spectral conditions basically as in (A) but 10000 scans per spectrum. (C) [δ-$^2H_3$]Leucine, spectral conditions basically as in (A) but 7200 scans per spectrum. (D) [$\alpha,\beta,\gamma,\gamma',\delta$-$^2H_{10}$]Isoleucine, spectral conditions basically as in (A) but 1000 scans per spectrum. τ_1 values are given at the left of the spectra in milliseconds.

Table IV: Experimental Deuterium NMR Quadrupole Splittings (QS), Spin-Lattice Relaxation Times (T_1), and Computed Correlation Times (τ_c) for Methyl Rotation in [γ-$^2H_6$]Valine-, [β,γ-$^2H_4$]Threonine-, and [δ-$^2H_3$]Leucine-Labeled Bacteriorhodopsin in the Purple Membrane of *H. halobium* R_1[a]

[γ-$^2H_6$]valine				[β,γ-$^2H_4$]threonine				[δ-$^2H_3$]leucine				[$\alpha,\beta,\gamma,\gamma',\delta$-$^2H_{10}$]isoleucine			
temp (°C)	QS[b] (kHz)	T_1 (ms)	τ_c (ps)	temp (°C)	QS[b] (kHz)	T_1 (ms)	τ_c (ps)	temp (°C)	QS[b] (kHz)	T_1 (ms)	τ_c (ps)	temp (°C)	QS[b] (kHz)	T_1 (ms)	τ_c (ps)
37	36.5	58	49	37	38	69.3	40	54	31	66.4	39	37	37	99.8	29
0	38.0	32.4	87	30	38	66.2	42	26	32	47.1	55	29	37	93.3	31
−30	39.0	18.6	150	24	38	50.5	56	−3	35	29.9	96	20	37	81.9	35
−59	40.0	10.1	280	9	38	37.4	76	−24	36	17.9	162	3	37	63.5	45
−159	40.0	4.07	740	3	38	26.9	108	−44	37	11.6	250	−11	37.5	53.9	53
				−18	38	17.7	160					−33	38	34.7	83
				−30	39	15.9	180								
				−38	39	13.7	220								
				−47	39	11.6	250								

[a] Data obtained by using an inversion recovery quadrupole echo sequence at 8.45 T (corresponding to a ^2H resonance frequency of 55.3 MHz) as described in the text. T_1 and τ_c accuracies are about ±10%. See Figures 6 and 7 for typical signal to noise ratios and Arrhenius plots. [b] Obtained from a spectral simulation; error is about ±2.5%.

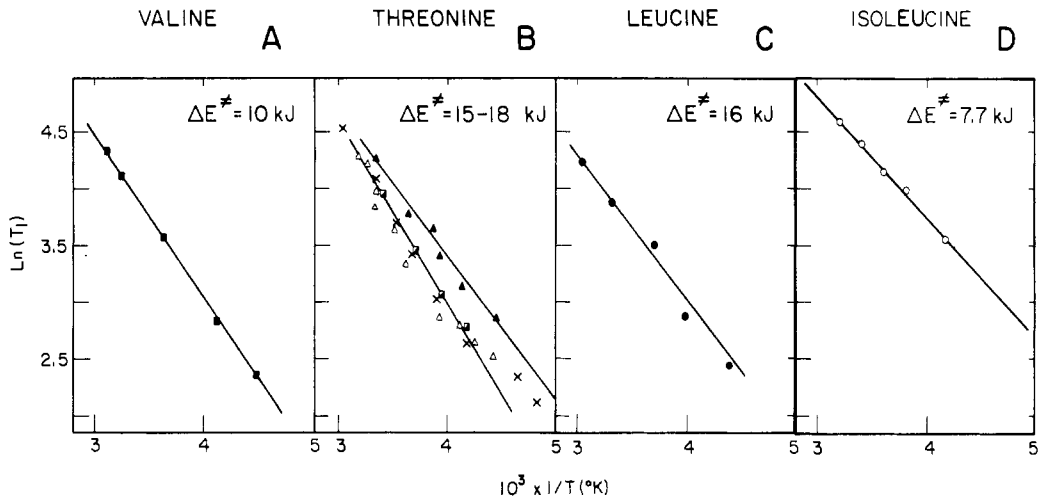

FIGURE 7: Arrhenius plots of spin–lattice relaxation times for Val-, Thr-, Leu-, and Ile-labeled purple membranes of Figure 6. (A) Val, $\Delta E^{\ddagger}$ = 10 ± 1 kJ; (B) Thr: (Δ) native, (▲) lyophilized, (box right solid) rehydrated, (×) C-terminal 10 residues removed, $\Delta E^{\ddagger} \approx$ 15–18 kJ; (C) Leu, $\Delta E^{\ddagger}$ = 15.6 ± 1.5 kJ; (D) Ile, $\Delta E^{\ddagger}$ = 7.7 ± 1 kJ.

rise to axially asymmetric ($\eta \sim 1$) powder patterns with quadrupolar splittings slightly narrower that 40 kHz (Batchelder et al., 1982). In addition to the ~40-kHz powder pattern, all the ^2H spectra of purple membranes display an isotropic central component that we believe is due to residues on the surface of the membrane undergoing fast large amplitude reorientation (M. A. Keniry et al., unpublished results).

The presence of side-chain hopping of the methyl-containing amino acid residues in the protein raises the question as to whether the theoretical model is still valid for extracting correlation times of methyl groups in bacteriorhodopsin. Batchelder et al. (1982) calculate that hops at a rate of $\sim 10^4$–10^6 s^{-1} are sufficient to produce these axially asymmetric spectra. A motion at this rate is far from the Larmor frequency and would not be very efficient for relaxation. Moreover, if this motion were significant in the relaxation of the methyl deuterons, we would expect a significant deviation from linearity in the Arrhenius plots, as was observed in DL-methionine (Keniry et al., 1983), especially since this motion is in the slow regime ($\omega_0\tau_c \gg 1$) and so would have a slope that is opposite to that caused by methyl rotation in the fast limit ($\omega_0\tau_c \ll 1$). Inspection of the Arrhenius plots of [γ-$^2H_6$]valine-, [δ-$^2H_3$]leucine-, and [$\alpha,\beta,\gamma,\gamma',\delta$-$^2H_{10}$]isoleucine-labeled purple membranes (Figure 7) shows only straight lines with slopes characteristic of the fast motion. Thus, we believe that methyl reorientation is the dominant relaxation mechanism of these amino acids in bacteriorhodopsin.

For [β,γ-$^2H_4$]threonine-labeled purple membrane, however, there appears to be a slight curvature of the Arrhenius plot in Figure 7, which contains the results of 10 spin–lattice relaxation time determinations on the native membrane over the temperature range 37 to −47 °C. Such behavior is not seen with the free amino acid (Figures 2 and 3). In the high-temperature limit (≳10 °C), $\Delta E^{\ddagger}$ is *apparently* lower (≈12 kJ). We observe the same behavior when the 10 C-terminal residues are cleaved, a procedure that results in reduction of the intensity of the isotropic component, centered at 0 kHz in the spectra, and immobilization of many surface residues (M. A. Keniry et al., unpublished results). The origin of this result is not clear at present. It may be due simply to a distribution of correlation times, or to the presence of a T_1 minimum, or it may be linked to the freezing of water in the system with resulting structural changes around the threonine side chains. The results of neutron diffraction experiments and model building (Engelman & Zaccai, 1980) suggest that most threonine residues are unusual in that they are located in a central, polar "pore" in the bacteriorhodopsin molecule, while the valines and apparently many leucines and isoleucines lie on the outside of the bacteriorhodopsin molecule, where they are associated with lipid. Such a pore location for threonine could make the threonine ^2H relaxation sensitive to the phase state of the solvent water, and the results of Figure 7 do indicate that there is a substantial increase in T_1 on water removal, with a decrease in T_1 following rehydration. At this

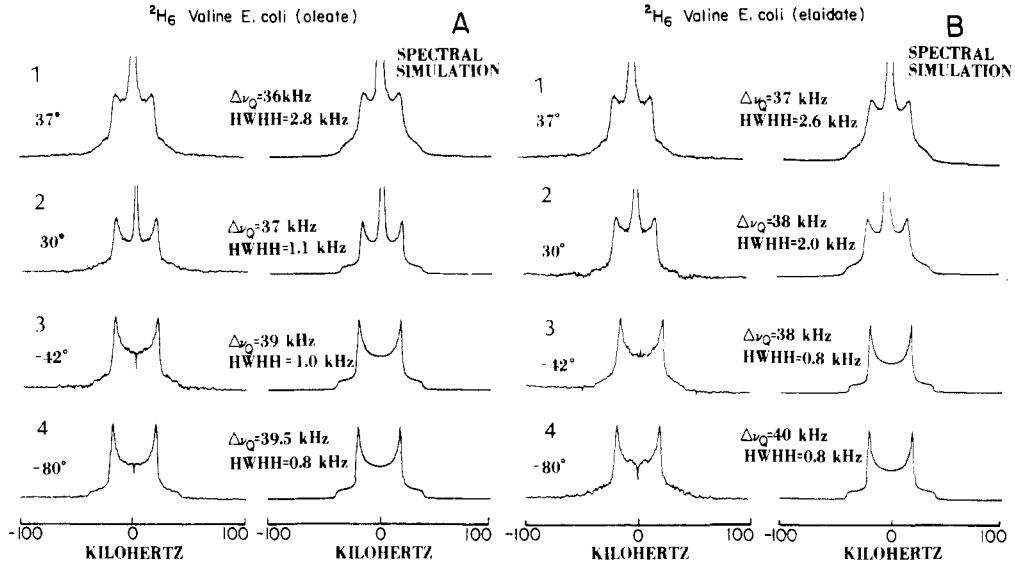

FIGURE 8: Typical experimental spectra, and spectral simulations, of [γ-$^2H_6$]valine-labeled *E. coli* cell membranes enriched with oleate or elaidate. All spectra were obtained at 32.9 MHz (corresponding to a magnetic field strength of 5.0 T) by using a quadrupole echo pulse sequence with the following parameters: 3-μs 90° pulse widths, $\tau_1 = \tau_2 = 80$ μs, 200-kHz digitization rate, 2048 data points, line broadening = 500 Hz, and typically 4000 accumulations per spectrum at a recycle time of between 50 and 500 ms. (A) Oleate-enriched membranes. (B) Elaidate-enriched membranes. Spectral simulations were carried out as described in the text, and the quadrupole splittings (QS, kilohertz) and line widths (HWHH, in kilohertz) are given in the figure. Temperatures are shown in degrees centrigrade. The poorer agreement between theory and experiment in the wings of the spectra may be attributed to power falloff.

time, however, the origins of this (weak) nonlinear Arrhenius behavior remain obscure.

The results in Table IV indicate that with the exception of isoleucine, the correlation times of all amino acid methyl groups are quite similar in the purple membrane at 37 °C (i.e., 45 ± 10 ps). This is in marked contrast to the trend observed for amino acids in the zwitterionic crystal lattice of increased motion with increasing distance from the α-carbon. The observed correlation times may reflect the looser, more flexible nature of the membrane protein as compared to the zwitterionic crystal lattices of these methyl-containing amino acids. The greater degrees of freedom in the protein as well as the more irregular packing compared to the crystal lattice make it likely that the methyl groups are in more similar environments. The more flexible nature of the membrane protein compared to the zwitterionic lattice is also supported by the activation energies for methyl group rotation in labeled bR (Table III), which except for threonine are much lower than in the zwitterionic lattice. Despite the lower activation energy in the membrane protein, however, the correlation times overall are quite similar to those in the zwitterionic crystal lattice. Again, we must look to activation entropies for our answer. With the exception of threonine, which has an unusual behavior in the purple membrane, all the activation entropies are more negative in the labeled purple membrane compared to the zwitterionic lattice. This compensates for the effect of the lower activation energy and results in comparable correlation times in the two systems.

Protein Dynamics: Escherichia coli. The above results indicate that the rates of motion of valine, threonine, leucine, and isoleucine in polycrystalline amino acids are quite similar to those when incorporated into the purple membrane of *H. halobium*. On this basis, the purple membrane appears to be "crystalline" in nature. The purple membrane is, however, atypical in its protein to lipid ratio (and lipid composition) since it contains ~80 wt % protein (bacteriorhodopsin) and only ~20 wt % of (isoprenoid) lipid. We felt that other cell membranes with higher lipid to protein ratios might have measurably different dynamical behavior (on the average); thus, we incorporated our selectively deuterated amino acids

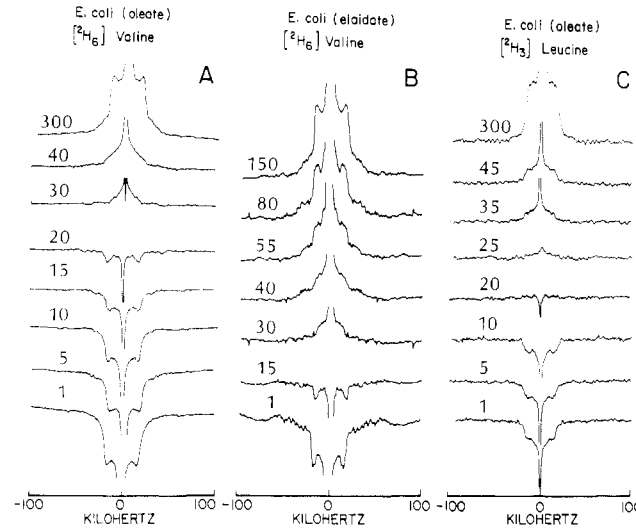

FIGURE 9: Partially relaxed deuterium Fourier transform NMR spectra of *E. coli* cell membranes containing specifically deuterated amino acids. (A) [γ-$^2H_6$]Valine labeled, oleate enriched, at 5.0 T (corresponding to a ^2H resonance frequency of 32.9 MHz). These membranes exhibited a sharp endotherm at ~22 °C: 4000 scans per spectrum. Spectral conditions for all spectra in this figure are basically the same as those in Figure 6. (B) [γ-$^2H_6$]Valine labeled, elaidate enriched, at 5.0 T. These membranes had a broad endotherm centered at about 35 °C: 4000 scans per spectrum. (C) [δ-$^2H_3$]Leucine labeled, oleate enriched, at 8.45 T (corresponding to a ^2H resonance frequency of 55.3 MHz): 3000 scans per spectrum. τ_1 values are indicated on the figure in milliseconds.

into the cell membranes of *E. coli*. Our preparation contains ~80% inner membrane.

We show in Figures 8 and 9 ^2H FT and PRFT NMR spectra of [γ-$^2H_6$]valine-labeled *E. coli* TS1 (a fatty acid auxotroph) enriched with either oleic (*cis*-octadec-9-enoic) or elaidic (*trans*-octadec-9-enoic) acid, together with similar deuterium NMR spectra of *E. coli* ATCC 23783 (a leucine auxotroph) grown on [δ-$^2H_3$]leucine and enriched with oleic acid. Differential scanning calorimetry of the oleate- and elaidate-enriched valine-labeled membranes (kindly carried out for us by Dr. R. N. McElhaney, University of British

Table V: Experimental Deuterium NMR Spin-Lattice Relaxation Times (T_1) and Computed Methyl Group Correlation Times (τ_c) for [γ-$^2H_6$]Valine in Elaidate- and Oleate-Enriched *E. coli* Cell Membranes and for [δ-$^2H_3$]Leucine in Oleate-Enriched Membranes[a]

[γ-$^2H_6$]valine, elaidate[b]			[γ-$^2H_6$]valine, oleate[c]			[δ-$^2H_3$]leucine, oleate		
temp (°C)	T_1[d] (ms)	τ_c (ps)	temp (°C)	T_1[d] (ms)	τ_c (ps)	temp (°C)	T_1[e] (ms)	τ_c (ps)
37	42.0	68	37	41.0	68	37	69.6	41
4	31.9	87	4	30.6	92	15	42.7	68
−20	19.9	140	−20	20.9	130	−2	30.1	96
−42	18.6	150	−42	14.3	200	−29	16.3	180
−60	7.2	400	−60	7.8	380	−54	6.7	460
−80	5.4	550	−80	5.1	580			

[a] Data obtained as described in the text. Accuracies in T_1 and τ_c are about ±10%. See Figures 8 and 9 for typical signal to noise ratios. [b] Membranes exhibited a broad lipid gel to liquid-crystal phase transition temperature centered at ~35 °C. [c] Membranes exhibited a narrow lipid gel to liquid-crystal phase transition centered at ~22 °C. [d] Data obtained at 5.0 T, corresponding to a ^2H resonance frequency of 32.9 MHz. [e] Data obtained at 8.45 T, corresponding to a ^2H resonance frequency of 55.3 MHz.

Table VI: Calculated Methyl Group Correlation Times at Room Temperature for Several Amino Acid Residues Incorporated into Various Biological Systems[a]

	alanine	valine	threonine	leucine	isoleucine	methionine
amino acid crystal	30–1500	150	60	60	18	5
alkaline phosphatase crystal[c]	nm[b]	85	nm[b]	90	nm[b]	nm[b]
H. halobium	nm[b]	65	56	60	35	nm[b]
E. coli	nm[b]	80	nm[b]	65	nm[b]	nm[b]
BPTI[d]	50	50	50	50	5–50	14

[a] τ_c values are in picoseconds. [b] Not measured. [c] Microcrystals of a biosynthetically enriched protein from an overproducing strain of *E. coli* (S. Schramm, J. A. Nichols, and E. Oldfield, unpublished results). [d] Bovine pancreatic trypsin inhibitor, from Ribeiro et al. (1980).

Columbia) revealed a sharp endotherm for the oleate-enriched membranes centered 22 °C (the growth temperature of the cells was 37 °C). Notably, however, there are no apparent effects of the lipid phase state on the ^2H T_1 results, as shown in Figure 9 and Table V.

The results for the [γ-$^2H_6$]valine- and [δ-$^2H_3$]leucine-labeled membranes (Figures 8 and 9), when analyzed as discussed previously, yield correlation times (τ_c) and activation energies (ΔE^*) very similar to those reported above for the purple membrane of *H. halobium* as shown in Tables III–V. For example, τ_c values for valine- and leucine-labeled *E. coli* at 37 °C are ~70 ± 10 ps, compared to ~50 ± 10 ps for bacteriorhodopsin; at −30 °C, the corresponding values are 160 ± 20 ps for valine- and leucine-labeled *E. coli*, compared to ~160 ± 20 ps for bacteriorhodopsin. In addition, the activation energies for methyl rotation are, within experimental error, the same in the two types of membrane (Table III): 9.6 and 14.7 kJ, respectively, for valine- and leucine-labeled *E. coli* compared to 10.0 and 15.6 kJ in bacteriorhodopsin.

These results clearly indicate that on the average the rates and types of motion of the valine and leucine side chains in these two very different membrane proteins are remarkably similar. By contrast, there is no observable effect of lipid composition, or of lipid phase state, on our ^2H NMR observations. This is presumably the result of the small size of the valine side chain, which will be protected from interactions with lipid by larger neighboring amino acid residues, together with, of course, the fact that on the average only a few residues in these large, globular membrane proteins will be undergoing intermolecular contacts with neighboring lipid (or protein) molecules. It may, however, be possible to see the effects of membrane fluidity on side-chain dynamics when using amino acids having larger side chains, especially in reconstituted systems with relatively small proteins.

An analysis of the dynamics of methyl-containing amino acids within an integral membrane would not be complete without a comparison with the dynamics of these amino acids in globular proteins. In Table VI, we compare the correlation times of the methyl rotor in the amino acids alanine, valine, threonine, leucine, and isoleucine in the crystalline form, in the membranes of *H. halobium* and *E. coli*, in a crystalline protein, and in the water-soluble, globular protein bovine pancreatic trypsin inhibitor. The correlation times are remarkably similar, considering the diverse environments in which these methyl groups reside. Valine, theonine, and leucine have correlation times in the range 50–90 ps at room temperature, indicating a probable similarity of microenvironment. Alanine, except for the remarkably high correlation time in the zwitterionic crystalline form, may also be classified with valine, threonine, leucine, and isoleucine. Methionine is atypical among the other amino acids because of the short correlation time seen in the crystalline amino acid and in BPTI. The presence of a large heteroatom and fewer bulky substituents in the side chain allow rapid methyl rotation and other side-chain motions at room temperature and above (Keniry et al., 1983).

Conclusions

The results in this paper represent our first attempts at determing the rates and types of motion of amino acids side chains in amino acid crystals, and in membrane proteins, by using solid-state NMR relaxation techniques. Activation energies and correlation times are all remarkably similar and are consistent with fast methyl rotation being the dominant source of ^2H spin–lattice relaxation for [β-$^2H_3$]alanine, [γ-$^2H_6$]valine, [β,γ-$^2H_4$]threonine, [δ-$^2H_3$]leucine, and [$\alpha,\beta,\gamma,\gamma',\delta$-$^2H_{10}$]isoleucine. Observation of a predicted T_1 minimum with alanine is strong evidence for the basic correctness of the motional model. Additional side-chain motions may contribute to the ^2H line shape and line breadth of valine, leucine, and isoleucine in membranes, especially at higher temperatures, but these motions are relatively slow and/or small in amplitude. The lipid phase state in the membranes studied does not greatly influence the motions of most amino acid side chains.

In other solid proteins and amino acids, motions other than methyl–C_3 rotation may contribute substantially to relaxation. For example, in the amino acid L-[ϵ-$^2H_3$]methionine, we find (Keniry et al., 1983) at low temperatures ($\lesssim$−40 °C) that relaxation is dominated by methyl rotation, but at higher

temperatures, a new fast motional process is apparent, and considerable changes in *both* line shape and T_1 are observed. Similar unusual behavior is also observed in microcrystals of myoglobin (Keniry et al., 1983).

Acknowledgments

We thank Catherine M. Flynn, Bernard Montez, Julie A. Nichols, and Joe Vandenbranden for help with sample preparation and characterization, Dr. John Cronan for the gift of *E. coli* TS1, Dr. R. N. McElhaney for calorimetric measurements on *E. coli* membranes, Suzanne E. Schramm for her unpublished results on *E. coli* alkaline phosphatase crystals, and Dr. Attila Szabo and Dr. Dennis Torchia for valuable discussions and a preprint of their manuscript.

Registry No. L-Alanine, 56-41-7; DL-valine, 516-06-3; DL-threonine, 80-68-2; L-leucine, 61-90-5; L-isoleucine, 73-32-5.

References

Alla, M., Eckman, R., & Pines, A. (1980) *Chem. Phys. Lett. 71*, 148–151.

Anderson, J. E., & Slichter, W. P. (1965) *J. Phys. Chem. 69*, 3099–3104.

Andrew, E. R., Hinshaw, W. S., Hutchins, M. G., Sjoblom, R. O. I., & Canepa, P. C. (1976) *Mol. Phys. 32*, 795–806.

Andrew, E. R., Gaspar, R., Jr., & Vennart, W. (1978) *Biopolymers 17*, 1913–1925.

Andrew, E. R., Bryant, D. J., & Cashell, E. M. (1980) *Chem. Phys. Lett. 69*, 551–554.

Batchelder, L., Sullivan, C. E., Jelinski, L. W., & Torchia, D. A. (1982) *Proc. Natl. Acad. Sci. U.S.A. 79*, 386–389.

Batchelder, L. S., Niu, C. H., & Torchia, D. A. (1983) *J. Am. Chem. Soc. 105*, 2228–2231.

Bloembergen, N. (1949) *Physica (Amsterdam) 15*, 386–426.

Davis, J. H., Jeffrey, K. R., Bloom, M., Valic, M. I., & Higgs, T. P. (1976) *Chem. Phys. Lett. 42*, 390–394.

Engelman, D. M., & Zaccai, G. (1980) *Proc. Natl. Acad. Sci. U.S.A. 77*, 5894–5898.

Fodor, P. J., Price, V. E., & Greenstein, J. P. (1949) *J. Biol. Chem. 178*, 503–509.

Glasstone, S., Laidler, P. J., & Eyring, H. (1941) *The Theory of Rate Processes*, McGraw-Hill, New York.

Jelinski, L. W., Sullivan, C. E., Batchelder, L. S., & Torchia, D. A. (1980) *Biophys. J. 10*, 515–529.

Kang, S. Y., Gutowsky, H. S., Hsung, J. C., Jacobs, R., King, T. E., Rice, D., & Oldfield, E. (1979a) *Biochemistry 18*, 3257–3267.

Kang, S. Y., Gutowsky, H. S., & Oldfield, E. (1979b) *Biochemistry 18*, 3268–3272.

Karplus, M., & McCammon, J. A. (1981) *CRC Crit. Rev. Biochem. 9*, 293–349.

Keniry, M., Rothgeb, T. M., Smith, R. L., Gutowsky, H. S., & Oldfield, E. (1983) *Biochemistry 22*, 1917–1926.

Kinsey, R. A., Kintanar, A., & Oldfield, E. (1981a) *J. Biol. Chem. 256*, 9028–9036.

Kinsey, R. A., Kintanar, A., Tsai, M.-D., Smith, R. L., Janes, N., & Oldfield, E. (1981b) *J. Biol. Chem. 256*, 4146–4149.

Levy, G., & Peat, I. (1975) *J. Magn. Reson. 18*, 500–521.

McCall, D. W., & Douglass, D. C. (1963) *Polymer 4*, 433–444.

Oldfield, E., & Rothgeb, T. M. (1980) *J. Am. Chem. Soc. 102*, 3635–3637.

Ribiero, A. A., King, R., Restivo, C., & Jardetzky, O. (1980) *J. Am. Chem. Soc. 102*, 4040–4051.

Sato, M., Okawa, K., & Akabori, S. (1957) *Bull. Chem. Soc. Jpn. 30*, 937–938.

Schajor, W., Pislewski, N., Zimmerman, H., & Haeberlen, U. (1980) *Chem. Phys. Lett. 76*, 409–412.

Schramm, S. E., & Oldfield, E. (1983) *Biochemistry 22*, 2908–2913.

Spiess, H. W., & Sillescu, H. (1981) *J. Magn. Reson. 42*, 389–394.

Torchia, D. A., & Szabo, A. (1982) *J. Magn. Reson. 49*, 107–121.

Vogel, H. J., & Bonner, D. M. (1956) *J. Biol. Chem. 218*, 97–106.

Wallace, B. A., & Henderson, R. (1982) *Biophys. J. 39*, 233–239.

Williams, R. J. P. (1978) *Proc. R. Soc. London, Ser. B 200*, 353–389.

Zaripov, M. R. (1973) in *Radiospecktroskopiya* (Kozyrev, B. N., Ed.) Moscow, pp 193–229; English Transl., British Library Lending Division, RTS 9205, 30 pp.